Research Article | Vol. 25, No. 9 | 1 May 2017 | OPTICS EXPRESS 10685

Optics EXPRESS

Homodyne-like detection for coherent state-discrimination in the presence of phase noise

MATTEO BINA,[1] ALESSIA ALLEVI,[2] MARIA BONDANI,[3] AND STEFANO OLIVARES[1,*]

[1] *Quantum Technology Lab, Department of Physics, University of Milan, via Celoria 16, I-20133 Milano, Italy*
[2] *Department of Science and High Technology, University of Insubria and CNISM UdR Como, Via Valleggio 11, 22100 Como, Italy*
[3] *Institute for Photonics and Nanotechnologies, CNR, and CNISM UdR Como, Via Valleggio 11, 22100 Como, Italy*
[*] *stefano.olivares@fisica.unimi.it*

Abstract: We propose a homodyne-like detection scheme involving photon-number-resolving detectors to discriminate between two coherent states affected by either uniform or gaussian phase noise. A proof-of-principle experiment is performed employing two hybrid photodetectors, whose outputs are used in post processing to calculate the shot-by-shot photon-number differences. The performance of the strategy is quantified in terms of the error probability in discriminating the noisy coherent signals as a function of the characteristic noise parameters.

OCIS codes: (270.5290) Photon statistics; (270.5565) Quantum communications; (060.4510) Optical communications.

References and links

1. S. Wallentowitz, and W. Vogel, "Unbalanced homodyning for quantum state measurements," Phys. Rev. A **53**, 4528–4533 (1996).
2. K. Banaszek, C. Radzewicz, K. Wódkiewicz, and J. S. Krasiński, "Direct measurement of the Wigner function by photon counting," Phys. Rev. A **60**, 674–677 (1999).
3. M. Bondani, A. Allevi, and A. Andreoni, "Wigner function of pulsed fields by direct detection," Opt. Lett. **34**, 1444–1446 (2009).
4. A. Allevi, S. Olivares, and M. Bondani, "Manipulating the non-Gaussianity of phase-randomized coherent states," Opt. Express **20**, 24850–24855 (2012).
5. S. Izumi, M. Takeoka, K. Wakui, M. Fujiwara, K. Ema, and M. Sasaki, "Optical phase estimation via coherent state and displaced photon counting," Phys. Rev. A **94**, 033842 (2016).
6. G. Puentes, J. S. Lundeen, M. P. A. Branderhorst, H. B. Coldenstrodt-Ronge, B. J. Smith, and I. A. Walmsley, "Bridging particle and wave sensitivity in a configurable detector of positive operator-valued measures," Phys. Rev. Lett. **102**, 080404 (2009).
7. K. Laiho, K. N. Cassemiro, D. Gross, and C. Silberhorn, "Probing the negative Wigner function of a pulsed single photon point by point," Phys. Rev. Lett. **105**, 253603 (2010).
8. L. Zhang, H. B. Coldenstrodt-Ronge, A. Datta, G. Puentes, J. S. Lundeen, X.-M. Jin, B. J. Smith, M. B. Plenio, and I. A. Walmsley, "Mapping coherence in measurement via full quantum tomography of a hybrid optical detector," Nat. Photon. **6**, 364–368 (2012).
9. G. Donati, T. J. Bartley, X.-M. Jin, M.-D. Vidrighin, A. Datta, M. Barbieri, and I. A. Walmsley, "Observing optical coherence across Fock layers with weak-field homodyne detectors," Nat. Commun. **5**, 5584 (2014).
10. S. Izumi, M. Takeoka, M. Fujiwara, N. Dalla Pozza, A. Assalini, K. Ema, and M. Sasaki, "Displacement receiver for phase-shift-keyed coherent states," Phys. Rev. A **86**, 042328 (2012).
11. C. R. Müller and Ch. Marquardt, "A robust quantum receiver for phase shift keyed signals," New J. Phys. **17**, 032003 (2015).
12. F. E. Becerra, J. Fan, G. Baumgartner, J. Goldhar, J. T. Kosloski, and A. Migdall, "Experimental demonstration of a receiver beating the standard quantum limit for multiple nonorthogonal state discrimination," Nat. Photon. **7**, 147–152 (2013).
13. F. E. Becerra, J. Fan, and A. Migdall, "Implementation of generalized quantum measurements for unambiguous discrimination of multiple non-orthogonal coherent states," Nat. Commun. **4**, 2028 (2013).
14. S. Olivares, S. Cialdi, F. Castelli, and M. G. A. Paris, "Homodyne detection as a near-optimum receiver for phase-shift-keyed binary communication in the presence of phase diffusion," Phys. Rev. A **87**, 050303 (2013).

#286274 https://doi.org/10.1364/OE.25.010685
Journal © 2017 Received 6 Feb 2017; revised 14 Mar 2017; accepted 18 Mar 2017; published 28 Apr 2017

Optics EXPRESS

15. M. Bina, A. Allevi, M. Bondani, and S. Olivares, "Phase-reference monitoring in coherent-state discrimination assisted by a photon-number resolving detector," Sci. Rep. **6**, 26025 (2016).
16. C. W. Helstrom, *Quantum Detection and Estimation Theory* (Academic, 1976).
17. J. G. Skellam, "The frequency distribution of the difference between two Poisson variates belonging to different populations," J. Roy. Statist. Soc. (N. S.) **109**, 296 (1946).
18. M. Bondani, A. Allevi, A. Agliati, and A. Andreoni, "Self- consistent characterization of light statistics," J. Mod. Opt. **56**, 226–231 (2009).
19. A. Andreoni and M. Bondani, "Photon statistics in the macroscopic realm measured without photon counters," Phys. Rev. A **80**, 013819 (2009).
20. A. Allevi, M. Bondani, and A. Andreoni, "Self-consistent phase determination for Wigner function reconstruction," J. Opt. Soc. Am. B **27**, 333–337 (2010).
21. K. Banaszek, A. Dragan, K. Wódkiewicz, and C. Radzewicz, "Direct measurement of optical quasi-distribution functions: Multimode theory and homodyne tests of Bell's inequalities," Phys. Rev. A **66**, 043803 (2002).
22. B. Efron, "Bootstrap methods: another look at the jackknife," Ann. Stat. **7**, 1–26 (1979).
23. BIPM, IEC, IFCC, ILAC, ISO, IUPAC, IUPAP, and OIML, *Evaluation of Measurement Data - Supplement 1 to the Guide to the Expression of Uncertainty in Measurement - Propagation of Distributions Using a Monte Carlo Method* (JCGM 101, 2008), http://www.bipm.org/utils/common/documents/jcgm/ JCGM_101_2008_E.pdf .
24. A. Allevi, S. Olivares, and M. Bondani, "Measuring high-order photon-number correlations in experiments with multimode pulsed quantum states," Phys. Rev. A **85**, 063835 (2012).
25. E. Diamanti, H.-K. Lo, B. Qi, and Z. Yuan "Practical challenges in quantum key distribution," npj Quantum Information **2**, 16025 (2016).
26. M. Ramilli, A. Allevi, V. Chmill, M. Bondani, M. Caccia, and A. Andreoni, "Photon-number statistics with silicon photomultipliers," J. Opt. Soc. Am. B **27**, 852–862 (2010).

1. Introduction

In this paper we propose a hybrid photodetection scheme [1–4] that takes advantage of the characteristics of both standard homodyne and photon-number-resolving (PNR) detectors. The detection apparatus exploits the usual interferometric scheme of homodyne detectors, using PNR detectors instead of pin-photodiodes to directly measure the photon numbers at the two outputs of the interferometer and evaluate their difference. The interferometric part of the detection scheme yields information on the phases, while PNR detectors provide direct access to the statistics of light, thus allowing the gain of much more information on the states than using, e.g., single-photon detectors [5]. At variance with other existing homodyne-like detection schemes [6–9], the employment of hybrid photodetectors, which are commercial detectors, allows us to explore a wide photon-number dynamic range (up to 30 photons). For this reason, the detection apparatus, though having an upper limit to the measurable light intensity, is also useful to investigate different regimes of local oscillator (LO) intensity.

In this work we apply the hybrid detector to a typical communication scheme based on coherent states. We use a strategy exploiting the difference of photocounts and leading to a discrimination error probability which approaches the minimum value allowed by quantum mechanics when phase noise affects the channel. This work completes and enriches the current research on optical communication schemes based on coherent states. In fact, during the last few years many efforts have been devoted to find optimal discrimination strategies, not only in the case of a binary coherent-state alphabet, but also in the presence of an M-ary system [10–13]. In particular, in Ref. [13] Becerra et al. consider the multiple discrimination of weak phase-shifted coherent states. The implemented receiver allows beating the standard quantum limit for discrimination, even if the procedure requires a high control degree of the relative phases and turns out to be very sensitive to phase fluctuations. As we will see, our strategy based on two-channel discriminator, i.e. the two outputs of the homodyne-like detection scheme, can successfully operate also in the presence of phase noise.

For what concerns the binary case, it has been recently demonstrated that, whenever a gaussian phase noise is present, a homodyne detection scheme realizes a discrimination strategy approaching the minimum error probability given by the Helstrom bound [14]. More recently, we have demonstrated that the use of PNR detectors is crucial for the estimation of phase drifts

Optics EXPRESS

in Kennedy-like receivers, in the regime of low-intensity LO and even in the presence of phase noise [15].

2. Homodyne detection with PNR detectors and state discrimination

The "imperfection" in a protocol aimed at discriminating between two non-orthogonal quantum states is quantified by the error probability P_e and depends on the employed measurement apparatus. Given two quantum states $\hat{\rho}_1$ and $\hat{\rho}_0$, with *a priori* probabilities η_1 and η_0, $\eta_1 + \eta_0 = 1$, the minimum error probability is given by the Helstrom bound [16]

$$P_e^{(H)} = \frac{1}{2}\Big[1 - Tr|\eta_1\hat{\rho}_1 - \eta_0\hat{\rho}_0|\Big]. \tag{1}$$

In our work we consider a standard scheme, in which a binary signal is encoded in two coherent states $\hat{\rho}_1 \equiv |\beta\rangle\langle\beta|$ and $\hat{\rho}_0 \equiv |-\beta\rangle\langle-\beta|$, $\beta \in \mathbb{R}$. Furthermore, we also assume that the propagation of the signals is affected by phase noise, whose effect can be described by the map

$$\hat{\rho}_k \mapsto \mathcal{E}(\hat{\rho}_k) = \int_{\mathbb{R}} \mathrm{d}\varphi\, f(\varphi)\hat{U}(\varphi)\hat{\rho}_k\hat{U}^\dagger(\varphi), \tag{2}$$

where $\hat{U}(\varphi) = \exp(-\mathrm{i}\varphi\hat{a}^\dagger\hat{a})$ is the phase-shift operator, $[\hat{a}, \hat{a}^\dagger] = \hat{\mathbb{I}}$ and $f(\varphi)$ is a weight function describing the phase noise distribution. In a uniform phase noise scenario $f(\varphi) = \gamma^{-1}$ if $\varphi \in [-\gamma/2, \gamma/2]$ and $f(\varphi) = 0$ otherwise. In the case of gaussian phase noise, $f(\varphi) = \mathcal{N}(\varphi; \sigma^2)$ is the normal distribution of mean value 0 and variance σ^2. In the presence of phase noise, by assuming $\eta_1 = \eta_0 = 1/2$, the Helstrom bound (1) is given by $P_e^{(H)} = \frac{1}{2}(1 - \mathrm{Tr}|\hat{\Lambda}|)$, where $\hat{\Lambda} = \frac{1}{2}[\mathcal{E}(\hat{\rho}_1) - \mathcal{E}(\hat{\rho}_0)]$.

To be decoded, the input state is mixed at a beam splitter (BS) of transmittance τ with the LO $|\alpha\rangle$, $\alpha \in \mathbb{R}$. The output modes $\hat{c}$ and $\hat{d}$ of the BS can be monitored by means of PNR detectors, giving access to the statistics of their photocounts n_c and n_d and, thus, of the difference $\Delta = n_c - n_d$, that is equivalent to a homodyne-like detection. In particular, the distribution of the aleatory variable Δ, with the two stochastic variables n_c and n_d described by Poisson distributions, having mean values μ_c and μ_d, is given by the Skellam distribution [17]

$$S_\Delta(\mu_c, \mu_d) = \mathrm{e}^{-\mu_c-\mu_d}\left(\frac{\mu_c}{\mu_d}\right)^{\frac{\Delta}{2}} I_\Delta(2\sqrt{\mu_c\mu_d}), \qquad \Delta \in \mathbb{Z}, \tag{3}$$

where $I_\Delta(x)$ is the modified Bessel function of the first kind. In the ideal case of the absence of phase noise, the mean values of the Poisson distributions for an input signal $|\beta\, e^{i\phi}\rangle$ are

$$\mu_c(\phi) = a_c^2 + b_c^2 + 2a_c b_c\cos(\phi) \quad \text{and} \quad \mu_d(\phi) = a_d^2 + b_d^2 - 2a_d b_d\cos(\phi)\ , \tag{4}$$

where we set $a_c^2 = \alpha^2(1-\tau)$, $a_d^2 = \alpha^2\tau$, $b_c^2 = \beta^2\tau$, and $b_d^2 = \beta^2(1-\tau)$. In order to define a discrimination strategy, let us assume that $\mu_c(0) > \mu_d(0)$ and $\mu_c(\pi) < \mu_d(\pi)$. Then we can use the following strategy: $\Delta > 0 \Rightarrow |\beta\rangle$ and $\Delta < 0 \Rightarrow |-\beta\rangle$ (for $\Delta = 0$ a random decision is made). Whenever $\Delta < 0$ ($\Delta > 0$) given the input $|\beta\rangle$ ($|-\beta\rangle$), an error in the inference occurs.

If we take into account phase noise, the mean numbers of photons at the outputs of the BS are still given by Eqs. (4), but with the substitution $\phi \to \phi - \varphi$. In this case, the overall error probability in the discrimination of $|\pm\beta\rangle$ is given by:

$$P_e^{(sk)} = \int_{\mathbb{R}} \mathrm{d}\varphi f(\varphi) p_e^{(sk)}(\varphi), \tag{5}$$

with:

$$p_e^{(sk)}(\varphi) = \frac{1}{2}\left[\sum_{\Delta=-\infty}^{-1} S_\Delta\Big(\mu_c(\varphi), \mu_d(\varphi)\Big) + \sum_{\Delta=1}^{+\infty} S_\Delta\Big(\mu_c(\varphi-\pi), \mu_d(\varphi-\pi)\Big) + S_0\right], \tag{6}$$

Optics EXPRESS

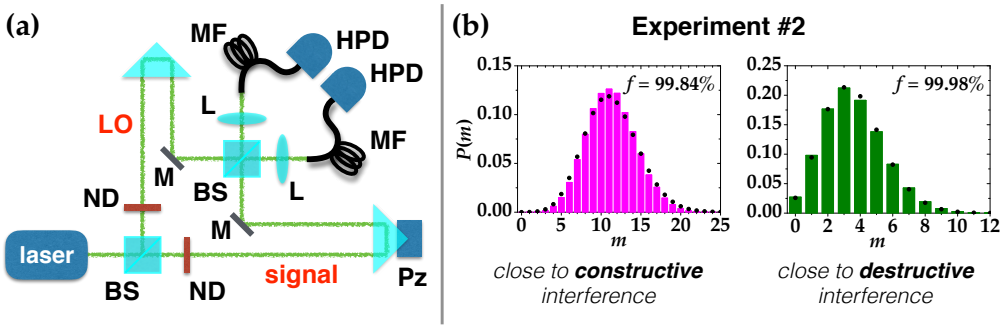

Fig. 1. (a) Sketch of the experimental setup. (b) Two typical photon-number distributions measured by the HPDs: experimental histograms, theoretical Poisson distribution (black dots), with the same mean value of the data, and the corresponding fidelities. See the text for details.

where S_0 is the value of the Skellam distribution for $\Delta = 0$, i.e. in the case of inconclusive measurement.

Given these assumptions, our main goal is to demonstrate that, by exploiting a detection scheme endowed with PNR detectors and performing the proposed homodyne-like strategy, it is possible to reach high-performance level in the discrimination protocol. As shown in [14], a standard homodyne scheme approaches this goal when phase noise affects the signals. In this case the error probability reads:

$$P_e^{(\mathrm{hd})} = \frac{1}{2}\left[\int_{-\infty}^{0} \mathrm{d}x \int_{\mathbb{R}} \mathrm{d}\varphi f(\varphi) p_{hd}(x;\beta;\varphi) + \int_{0}^{+\infty} \mathrm{d}x \int_{\mathbb{R}} \mathrm{d}\varphi f(\varphi) p_{hd}(x;-\beta;\varphi)\right], \tag{7}$$

where we introduced the homodyne probability distribution

$$p_{hd}(x;\pm\beta;\varphi) = \frac{1}{\sqrt{\pi}} \mathrm{e}^{-(x \mp \sqrt{2}\beta\cos\varphi)^2}, \tag{8}$$

in which the LO is a macroscopic coherent field.

3. Proof-of-principle experiment

In order to test the performance of our strategy, i.e. the employment of PNR detectors in a homodyne-like measurement with a low-intensity LO and in the presence of phase noise, we realized a proof-of-principle experiment.

As shown in Fig. 1(a), the second-harmonic pulses (5-ps-pulse duration) emitted at 523 nm by a mode-locked Nd:YLF laser regeneratively amplified at 500 Hz were sent to a Mach-Zehnder interferometer to get signal and LO. In order to set the intensities of the two fields, we inserted two variable neutral density filters (ND) in the two arms and we optimized the spatial and temporal superposition of signal and LO in order to get almost the best overlap admitted by the choice of the amplitudes and of the balancing (see below). The length of one arm of the interferometer was changed in steps by means of a piezoelectric movement (Pz) in order to modify the LO phase in the whole $2\pi-$range. The light at the two outputs of the second BS was collected by two multi-mode fibers (MF, 600-μm-core diameter) and sent to two hybrid photodetectors (HPD, mod. R10467U-40, Hamamatsu), which play the role of the PNR detectors. HPDs are commercial photodetectors, whose technology has been already addressed in Ref. [18]. The output of each detector was amplified (preamplifier A250 plus amplifier A275, Amptek), synchronously integrated over a 500-ns window (SGI, SR250, Stanford) and digitized (AT-MIO-16E-1, National Instruments). According to the model already presented in Ref. [19], the

Optics EXPRESS

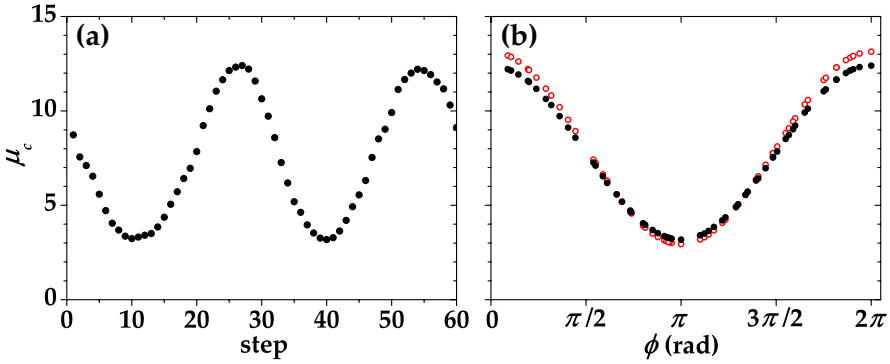

Fig. 2. Mean number of photons μ_c as a function of the step of (a) the piezoelectric movement and (b) of the relative phase ϕ (black dots). In both panels we use the same scale for vertical axis. We also report μ_c calculated according to Eq. (4) with $\tau = 0.5$ and the amplitudes of the signal, b, and LO, a, measured separately (red circles). Data refer to Experiment #2. See the text for details.

detection process consists of two steps: photodetection by the photocathode and amplification. The first process is described by a Bernoullian convolution, whereas the second one can be well approximated by the multiplication by a constant gain factor. We have already demonstrated that the value of the gain can be obtained by means of a self-consistent method [18] based on the very light to be measured. Once the value of the gain is determined, we have direct access to the shot-by-shot number of detected photons and can thus evaluate the statistical properties of the measured states.

In the present work we chose two different configurations: Experiment #1, in which we mixed a coherent signal with a LO of similar amplitude and Experiment #2, in which the intensity of the LO is much larger than that of the signal. We set 60 different piezo positions and for each one we saved 50 000 laser shots. Typical reconstructions of the photon-number statistics registered by each detector are shown in Fig. 1(b), from which it is possible to appreciate the wide dynamic range of HPDs. In particular, the data approximately correspond to the constructive (left) and destructive (right) interference conditions for Experiment #2. In both cases the experimental data well superimpose to the theoretical Poisson distributions evaluated with the experimental mean values. This is testified by the high values of fidelity $f = \sum_{m=0}^{\bar{m}} \sqrt{P(m)P_{\rm theo}(m)}$, where $P(m)$ and $P_{\rm theo}(m)$ are the experimental and theoretical distributions, respectively, and the sum is extended up to the maximum detected photon number, $\bar{m}$, above which the two distributions become negligible.

By exploiting the linearity of HPDs it is also possible to extract information about the phase [15, 20]. To explain the method we focus on the output mode $\hat{c}$. The mean number of detected photons μ_c, shown in Fig. 2(a) for Experiment #2, describes the interference pattern as a function of the piezo position. The relative phase ϕ between the two arms of the interferometer can be retrieved by suitably normalizing μ_c and by fitting the rescaled data with a cos function. In Fig. 2(b) μ_c is plotted as a function of ϕ (black dots). In the same plot, we also show the mean number of photons (red empty circles) calculated according to Eq. (4) by using the experimental values b and a of the signal and LO, separately measured. Given the experimental $\mu_c(\phi)$, it is possible to extract the effective portions of LO (a_c and a_d) and signal (b_c and b_d), both transmitted and reflected by the BS. In particular, by fitting these experimental data with (4), we obtain the effective values of the output coherent amplitudes in Experiment #1 ($a_c = 2.01$, $a_d = 2.07$, $b_c = 1.13$, and $b_d = 1.07$) and in Experiment #2 ($a_c = 2.74$, $a_d = 2.68$, $b_c = 0.87$, and $b_d = 0.85$).

To estimate the overlap between signal and LO, we evaluate the fringe visibility $v_{\rm exp} = (\mu_{\rm max} -$

Optics EXPRESS

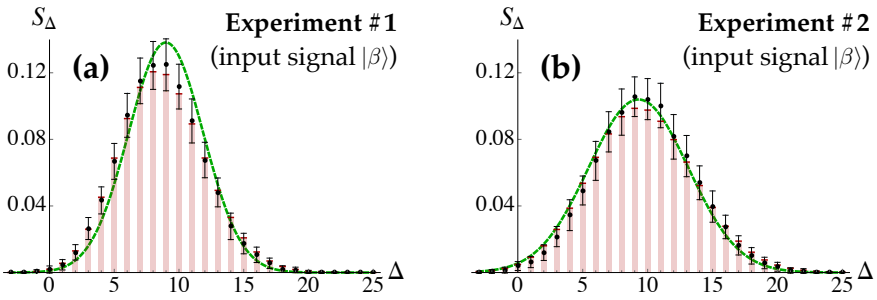

Fig. 3. Plots of $S_\Delta\big(\mu_c(0), \mu_d(0)\big)$ as a function of Δ, for both Experiment #1 (a) and Experiment #2 (b), with the choice $\phi = 0$, corresponding to the input $|\beta\rangle$. The fidelity between the data, averaged over $M = 100$ repetitions (dots), and the histograms, representing the theoretical previsions (3), are $f = 99.89\%$ for the Experiment #1 and $f = 99.73\%$ for the #2. For the sake of completeness, we also report the properly theoretical homodyne probability distribution (8) as a function of $x = \Delta/(\sqrt{2}\alpha)$ and suitably renormalized (green dashed line). See the text for details.

$\mu_{\min})/(\mu_{\max} + \mu_{\min})$. As an example, for the data in Fig. 2 (Experiment #2), the experimental visibility is 58%. Such a value must be compared to the expected theoretical visibility evaluated as $v_{\text{theo}} = 2a\,b/(a^2 + b^2)$, which is 63% for Experiment #2. By normalizing the value of v_{exp} to v_{theo}, the overlap of signal and LO can thus be calculated as $\xi = v_{\text{exp}}/(2 - v_{\text{exp}}) = 0.85$ [21], which is a good estimate of the mode matching between the two fields. In the following we show that, despite the non-unitary value of ξ, quasi-optimality in the state discrimination process can be achieved, in a robust way with respect to losses.

Once assigned a phase $\phi \in (0, 2\pi]$ to each piezo position, the set of output photocounts (and thus the corresponding differences Δ) given the input signal $|\beta\, e^{i\phi}\rangle$ and the LO $|\alpha\rangle$ can be obtained. The samples of detected photocounts from the mixtures of coherent states in Eq. (2), which are characterized by either uniform or gaussian phase noise, are retrieved by selecting and properly combining the data recorded at different phases. These prepared samples can be used to evaluate the error probability $P_e^{(sk)}$ in Eq. (5). In order to estimate the uncertainty of $P_e^{(sk)}$, we applied a bootstrap procedure [22, 23]. We randomly selected $N_{\text{s}} = 1\,000$ photocounts from the prepared samples, computed the differences Δ and evaluated $P_e^{(sk)}$ according to the discrimination strategy. Following the bootstrap prescription, we repeated such an operation $M = 100$ times and, then, retrieved a standard deviation of $P_e^{(sk)}$.

In Fig. 3, we show the probability distribution of the photocount differences Δ obtained for Experiment #1 (a) and #2 (b) when only $|\beta\rangle$ is sent, i.e. for $\phi = 0$. The experimental points and error bars represent the average and the standard deviation obtained by means of the bootstrap procedure. The theoretical expectations (histogram) given by the distributions (3), evaluated at the experimental values of $\mu_c(0)$ and $\mu_d(0)$, are well-superimposed to the experimental data, with fidelities $f \gtrsim 99\%$. In the same figure we also show the corresponding standard homodyne distribution (8) as a function of Δ, namely, $p_{hd}(\Delta/(\sqrt{2}\alpha); \pm\beta; \varphi)/(\sqrt{2}\alpha)$. The homodyne probability appears closer to the Skellam distribution in the Experiment #2, see Fig. 3(b), where the intensity of the LO, $|\alpha|^2$, is about 10 times larger than that of the signal, $|\beta|^2$. On the contrary, in the case of the Experiment #1 it is about 3.4 times, as also reported in Fig. 4.

4. Results

The experimental results are shown in Figs. 4(a)-(b) for the Experiment #1 and in Figs. 4(c)-(d) for the Experiment #2. The error probabilities have been obtained for different values of the

Optics EXPRESS

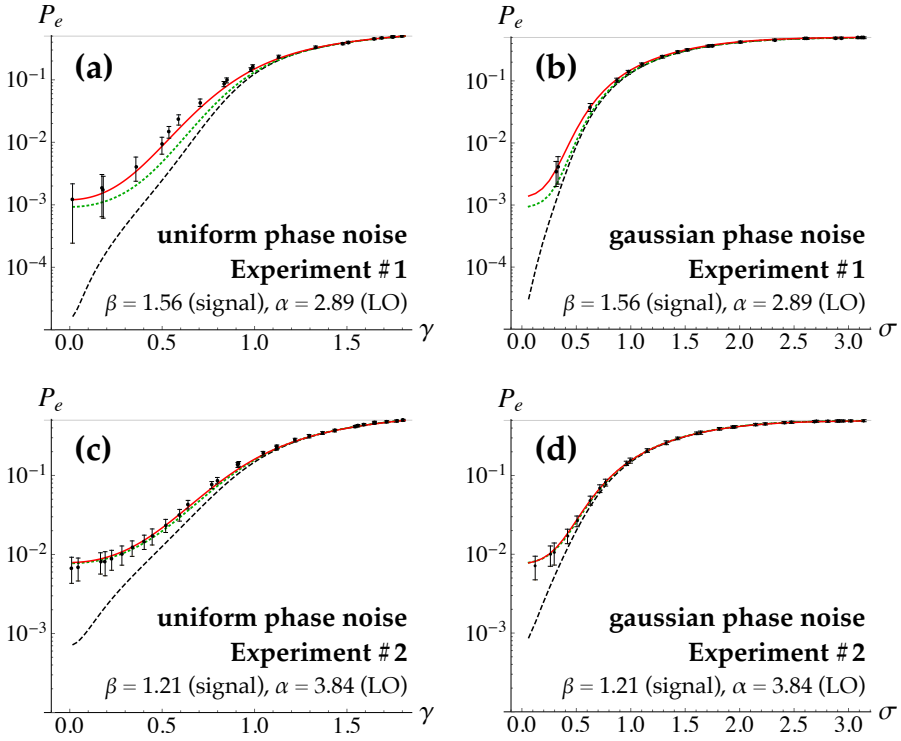

Fig. 4. Error probability (in logarithmic scale) obtained by the experimental homodyne-like photocount differences Δ (black dots with error bars) as a function of the uniform phase-noise parameter γ (a)-(c) and gaussian phase-noise one σ (b)-(d) for the Experiment #1 (a)-(b) and #2 (c)-(d), where β and α are the amplitudes of signal and LO, respectively [see Eq. (4)]. We also plot the theoretical prediction using the Skellam distribution (solid red lines), the corresponding theoretical standard homodyne detection (green dotted lines), given by Eq. (7), and the Helstrom bound (black dashed lines).

uniform noise parameter γ, and the gaussian noise standard deviation σ. The experimental results (error bars have been evaluated as described above) remarkably agree with the theoretical prediction (solid red curve) given by Eq. (6).

In Fig. 4 we also compare our discrimination strategy with the theoretical predictions of standard homodyne detection (green lines in the figures) based on pin-photodiodes (and same detected energy). As demonstrated in Ref. [14], standard homodyne approaches the Helstrom bound when the coherent signal is affected by phase noise. In both the considered experiments, we observe that the error probability provided by our discrimination strategy is very close to the homodyne one. The performance becomes almost the same when the amplitude of the LO is significantly larger than that of the signal, see Figs. 4(c)-(d), thus approaching the ultimate bound imposed by quantum mechanics. Moreover, the values of P_e are lower in Experiment #1 than in Experiment #2: this is simply due to the different amplitude values of the signal in the two cases and the higher the signal intensity the lower the error probability.

The obtained error probabilities display a different behavior when the two phase-noise models are employed. In order to make a fair comparison between them, we equate the variances of the two phase-noise distributions, thus obtaining the relationship $\sigma = \gamma/(2\sqrt{3})$ between the two noise parameters. From Fig. 5, it is clear that, for some values of the uniform noise parameter γ, the error probabilities corresponding to Eqs. (1) and (5) are below those obtained for the

Optics EXPRESS

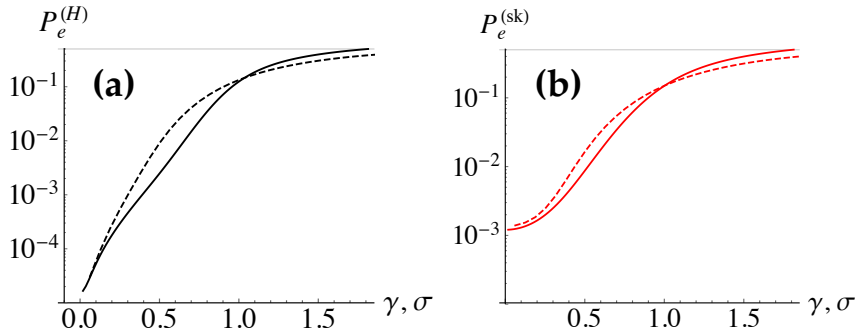

Fig. 5. Error probabilities $P_e^{(H)}$ (a) and $P_e^{(sk)}$ (b) for uniform (solid curves) and gaussian (dashed curves) phase noise, in Experiment #2. For a fair comparison we set $\sigma = \gamma/(2\sqrt{3})$.

gaussian-noise case.

5. Conclusions

We presented a two-channel coherent state discriminator, namely a homodyne-like detection scheme based on HPDs in the regime of low-intensity signals and LO. With respect to single-channel setups, which are usually very sensitive to phase noise, the increased complexity of our experimental scheme allowed us to obtain a discrimination error probability approaching the ultimate limits imposed by quantum mechanics also in the presence of phase noise. In our opinion, this feature represents a good advance towards the practical realization of optical communication channels, as they are typically affected by phase noise. In particular, we experimentally demonstrated that the effectiveness of our detection technique in addressing the shot-by-shot discrimination protocol is very similar to, and in some cases indistinguishable from, that of the standard homodyne technique. We characterized this discrimination strategy for both uniform and gaussian phase noise, showing that there are threshold values of the noise parameters for which the error probability is minimal. Our results testify how our scheme approaches the performance of standard homodyne detection, leading to the ultimate quantum limit (Helstrom bound) in the presence of phase noise. Moreover, our strategy also allows exploiting the advantages given by the photon-number resolving capability of HPDs. In particular, by detecting the photon statistics of the output signals, one can simultaneously assess the quantumness of the input states [24], thus paving the way, e.g. to the implementation of continuous-variable cryptographic schemes with nonclassical states [25], such as squeezed and sub-Poissonian states. In order to improve the quality of our detection scheme for other possible applications, now we are considering the use of the new generation of Si-photomultipliers [26] instead of HPDs.

Acknowledgments

SO thanks Matteo G. A. Paris for stimulating and useful discussions and Luca Sguera for his support in the early stage of this work.